

Supplementary Material for:

New mononuclear Dy(III) complex based on calix[4]arene ligand with two appended salicylideneamine groups decorated by azophenyl fragments: synthesis, crystalline assembly and slow magnetic relaxation behavior

Iuliia V. Strelnikova,^{a,b} Angelina A. Iova,^b Alexander S. Ovsyannikov,^{a,*} Daut R. Islamov,^c Igor A. Litvonov,^a Vladimir A. Lazarenko,^d Elizaveta S. Kulikova,^d Artem S. Bogomyakov,^e Meijin Lin,^f Ayrat G. Kiiamov,^b Svetlana E. Solovieva,^a Igor S. Antipin^b

^a *Arbuzov Institute of Organic and Physical Chemistry, FRC Kazan Scientific Center, Russian Academy of Sciences, Arbuzova 8 str, Kazan, 420088, Russian Federation*

^b *Kazan Federal University, Kremlevskaya 18 str, Kazan 420008, Russian Federation*

^c *Laboratory for structural analysis of biomacromolecules, FRC Kazan Scientific Center, Russian Academy of Sciences, Lobachevskogo 2/31 str., Kazan, 420111, Russian Federation*

^d *National Research Center "Kurchatov Institute", Academician Kurchatov 1 pl., Moscow, 123182, Russian Federation*

^e *International Tomography Center, Siberian Branch, Russian Academy of Sciences, Institutskaya 3a str., 630090 Novosibirsk, Russian Federation*

^f *College of Chemistry, Fuzhou University, Fuzhou, 350116, P. R. China*

** corresponding author:*

E-mail address: osaalex2007@ramble.ru

1. Experimental section

1.1. Materials and instrumentation

All chemicals were purchased from commercial suppliers and used without additional purification. Solvents were purified according to standard procedures.¹ *p-tert*-Butylcalix[4]arene (**1**) were synthesized following the reported procedure.² The distal substituted precursor *bis*-(2-aminoethoxy)-*p-tert*-butylcalix[4]arene was prepared as described earlier.³ Substance purity and reaction progress were monitored by TLC on Merck UV 254 plates and visualized by exposure to UV with a VL-6.LC lamp (Vilber, Marne-la-Vallée, France).

The ¹H and ¹³C NMR spectra were recorded on AVANCE IITM 400/100 MHz BRUKER BioSpin (Germany) with signals from residual protons of CDCl₃ as internal standard.

The High-Resolution Mass Spectra with ElectroSpray Ionization (HRESI MS) were obtained on an Agilent iFunnel 6550 Q-TOF LC/MS (Agilent Technologies, Santa Clara, CA, USA). Carrier gas: nitrogen, temperature 300 °C, carrier flow rate 12.1 × min⁻¹, nebulizer pressure

275 kPa, funnel voltage 3500 V, capillary voltage 500 V, total ion current recording mode, 100–3200 m/z mass range, scanning speed 7 spectra·s⁻¹.

The MALDI TOF mass spectra were recorded on an Ultraflex III TOF/TOF mass spectrometer (Bruker Daltonic GmbH, Bremen, Germany) operated in the linear mode with the registration of positively charged ions or negatively charged ions. A Nd:YAG laser ($\lambda = 355$ nm, repetition rate 100 Hz) was used. The mass spectrum was obtained with an accelerating voltage of 25 kV and an ion extraction delay time of 30 ns. The resulting mass spectrum was formed due to multiple laser irradiation of the crystal (50 shots). The metal target MTP AnchorChipTM was used. Portions (0.5 μ l) of a 1% matrix solution in acetonitrile and of a 0.1% sample solution in methanol were consecutively applied onto the target and evaporated. 2,5-Dihydroxybenzoic acid (DHB) was used as a matrix. The polyethylene glycol was used to calibrate the mass scale of the device. The data was obtained using the FlexControl program (Bruker Daltonik GmbH, Germany) and processed using the FlexAnalysis 3.0 program (Bruker Daltonik GmbH, Germany).

Infrared spectra (IR) of milled crystalline samples in KBr were recorded on a Tensor 27 Fourier-transform spectrometer (Bruker) in a range of 4000–400 cm⁻¹ with an optical resolution of 4 cm⁻¹ and an accumulation of 32 scans.

The X-ray powder diffraction pattern of quickly decomposing crystalline phase of **2-Dy** was studied at room temperature at the ‘Belok/XSA’ beamline of the Kurchatov synchrotron radiation source, equipped with a Rayonix SX165 two-dimensional CCD detector ($\lambda=0.7517$ Å).^{4,5} The measurements were carried out at room temperature in the transmission geometry, the detector was located at a distance of 250 mm from the sample and 18° tilt angle to maximize the angular range. The diffraction pattern was converted to the one-dimensional form I (2 θ) using azimuthal integration in the Dionis software,⁶ with the use of the certified LaB₆ (NIST SRM 660a) as polycrystalline standard.

A TGA/DSC NETZSCH (Selb, Germany) STA449 F3 was used for the thermal analysis (thermogravimetry/differential scanning calorimetry) in which the variation of the sample mass as a function of temperature and the corresponding heats are recorded. An approximately 15 mg sample was placed in an Al crucible with a pre-hole on the lid and heated from 25 to 500°C. The same empty crucible was used as the reference sample. High-purity argon was used with a gas flow rate of 50 mL/min. TGA measurement were performed at the heating rates of 5 K/min

Elemental analysis was performed on a EuroEA 3028-HT-OM Eurovector S.p.A. (Italy).

1.2. Synthesis of ligand 2

Compound **2** was synthesized by following the earlier reported method,⁷ but using the slightly modified protocol.

5-(Phenylazo)salicylaldehyde (0.34 g, 1.49 mmol) was added to a suspension of *bis*-(2-aminoethyl)-*p*-*tert*-butylcalix[4]arene (0.5 g, 0.68 mmol) in ethanol (20 ml), and the reaction mixture was stirred at room temperature for 10 h. The yellow precipitate was formed, filtered off, washed with cold ethanol (10 ml) and dried in vacuum, affording a pure product (0.48 g, 80%). ¹H NMR (600 MHz, CDCl₃) δ, ppm: 8.63 (2H, *s*, CHN), 7.92 (2H, *d*, ⁴*J*=2.5, H_{Ar}), 7.84 (2H, *dd*, ³*J*=8.9 Hz, ⁴*J*=2.5 Hz, H_{Ar}), 7.78-7.80 (4H, *m*, H_{Ar}), 7.41-7.43 (4H, *m*, H_{Ar}), 7.34-7.36 (2H, *m*, H_{Ar}), 6.90-6.92 (6H, *m*, H_{Ar}), 6.63 (4H, *s*, H_{Ar}), 6.60 (2H, *s*, OH), 4.22 (4H, *t*, ³*J*=5.2 Hz, CH₂), 4.16 (4H, *d*, ²*J*=13.0 Hz, CH), 4.08 (4H, *t*, ³*J*=5.2 Hz, CH₂), 3.19 (4H, *d*, ²*J*=13.0 Hz, CH), 1.22 (18H, *s*, *t*-Bu), 0.81 (18H, *s*, *t*-Bu). ¹³C NMR (600 MHz, CDCl₃) δ, ppm: 167.88, 165.04, 152.91, 150.52, 149.77, 147.27, 145.17, 141.59, 132.35, 130.43, 129.21, 127.92, 127.83, 127.19, 125.72, 125.16, 122.61, 118.50, 118.28, 74.89, 58.35, 34.00, 33.95, 31.85, 31.76, 31.07. HRESI-MS: observed *m/z* [M+H]⁺ = 1151.6419 (calculated *m/z* [M+H]⁺ = 1151.6374). IR (KBr, cm⁻¹) ν: 3427(*m*), 3047(*w*), 2958(*m*), 2868(*w*), 1635(*s*), 1438(*w*), 1462(*m*), 1286(*m*), 1194(*m*), 1110(*m*), 1049(*w*), 872(*w*), 766(*w*), 689(*w*). Elemental analysis found: C, 77.26 %; H, 6.56 %; N, 6.12 %, calc. for C₇₄H₈₂N₆O₆: C, 77.19; H, 7.18; N, 7.30.

1.3. Ligand characterization

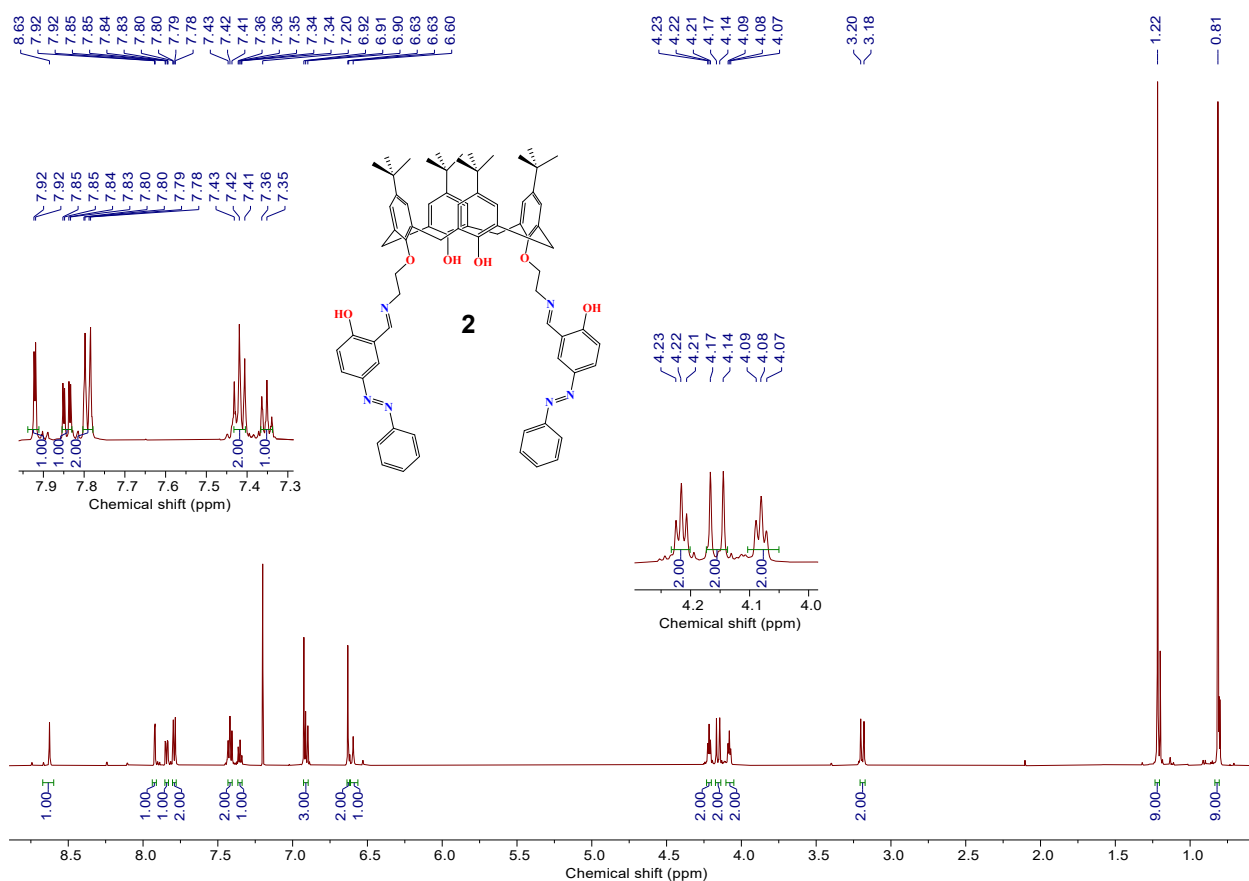


Figure S1. ^1H NMR spectrum for **2** (CDCl_3 , 400 MHz, 25 °C).

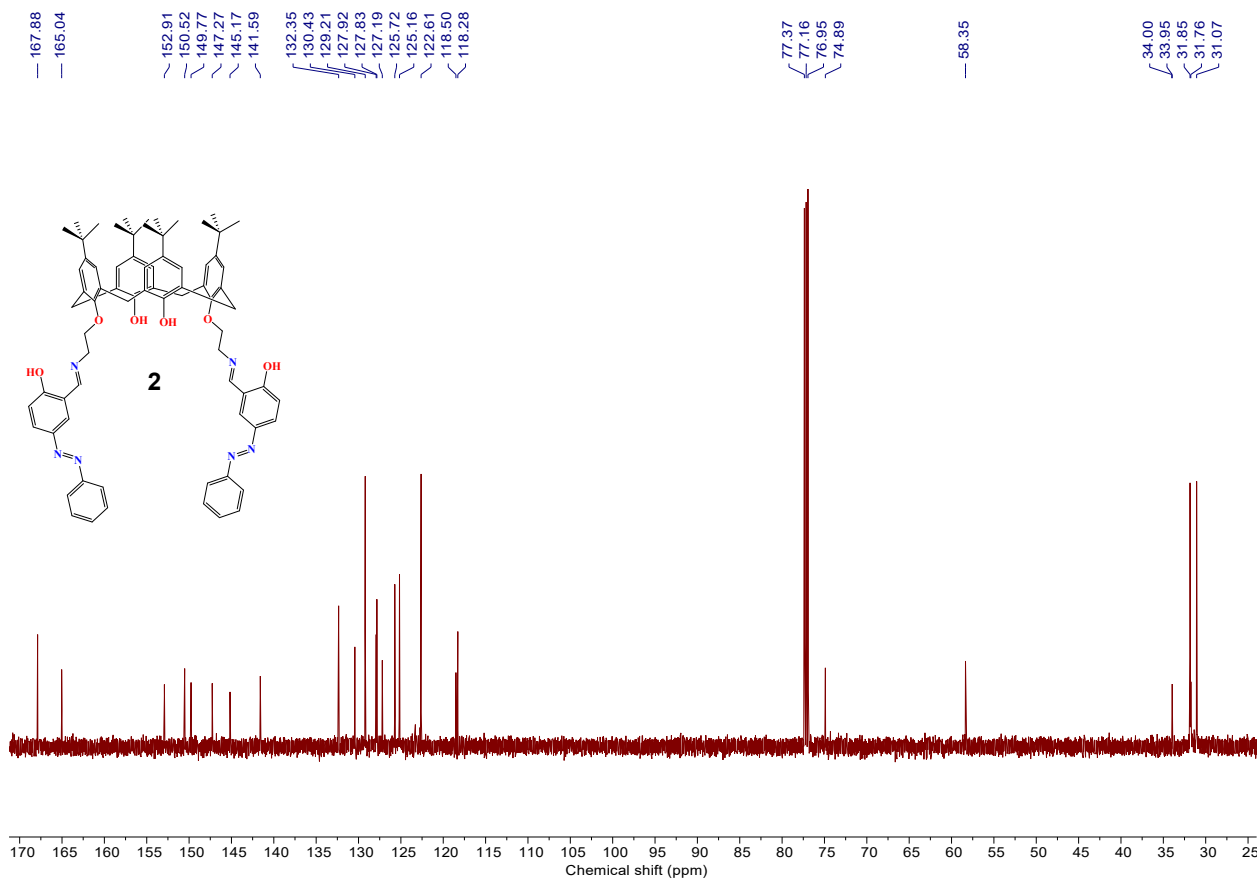


Figure S2. ^{13}C NMR spectrum for **2** (CDCl_3 , 100 MHz, 25 °C).

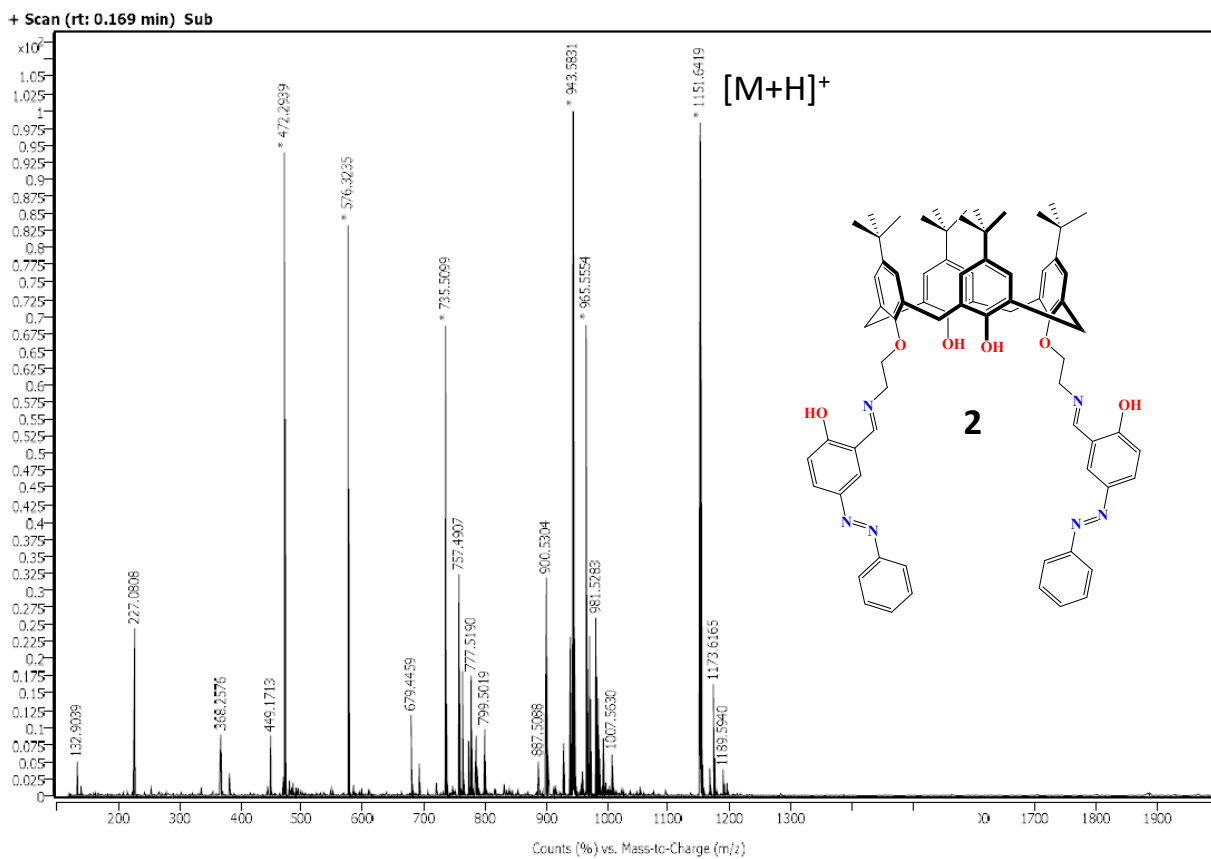


Figure S3. HRESI-MS spectrum for **2**.

1.3.2. Crystallization conditions for 2

2, [C₇₄H₈₂N₆O₆]: In a crystallization vial, to a solution of **2** (6 mg, 0.005 mmol) in CHCl₃ (2 ml) the MeOH was added (2 ml). The slow evaporation of the obtained mixture produced the formation of orange monocrystals, suitable for single-crystal X-ray diffraction, after 3 days.

1.4. Crystallization conditions for 2-Dy

2-Dy, [C₇₄H₇₈DyN₆O₆] CH₄O, H₂O : Compound **2** (50 mg, 0.044 mmol) with Dy(NO₃)₃·5H₂O (38.1 mg, 0.087 mmol) were dissolved in CH₂Cl₂/MeOH mixture (v/v = 1/1, 10 ml) followed by triethylamine addition (0.060 ml, 0.435 mmol). The reaction mixture was stirred at room temperature for 1 hour then filtered out. The orange monocrystals, suitable for X-ray diffraction, were obtained upon slow evaporation of the mother liquor at room temperature under aerobic conditions after one day. Yield: 45 mg, 77 %. MALDI TOF-MS: observed m/z [M-H]⁺ = 1310.9 (calculated m/z [M-H]⁺ = 1310.5). IR (ν_{max}/cm⁻¹): 3427(s), 3047(w), 2958(s), 2905(w), 2868(m), 1635(s), 1484(s), 1438(w), 1362(m), 1286(m), 1194(w), 1110(w), 921(w), 872(w), 766(w), 689(w). Elemental analysis found: C, 66.1 %; H, 6.25 %; N, 6.12 %, calc. for [C₇₄H₇₈DyN₆O₆] CH₄O, H₂O: 66.24 %; H, 6.23%; N, 6.18 %.

1.5. X-ray diffraction study

1.5.1. Details of the X-ray diffraction on single crystal experiments

Data set for **2** was collected on a Bruker D8 QUEST automatic three-circle diffractometer with a PHOTON III two-dimensional detector and an I μ S DIAMOND microfocus X-ray tube (λ [Mo K α] = 0.71073 Å) at cooling conditions. A single crystal of a suitable size is glued onto a glass thread in a random orientation. Data collection and indexing, determination and refinement of the unit cell parameters were carried out using the APEX2 software package.⁸ Empirical absorption correction based on the crystal shape, additional spherical correction and accounting for systematic errors were carried out using the SADABS program.⁹ The structures were solved by direct methods using SHELXT¹⁰ and refined by the full-matrix least-squares on F^2 using SHELXL.¹¹ Non-hydrogen atoms were refined in the anisotropic approximation. The positions of hydrogen atoms at carbon atoms were calculated geometrically and refined according to the “riding model”. Due to poor quality of crystals **2**, the correction of data sets at θ_{max} was applied based on the R_{merge} vs Resolution and I/σ vs Resolution plots (see below Figure SA). The 2θ angle ranges of $4.15 \leq 2\theta \leq 47^\circ$ was found to be the most suitable for the structure refinement in order to find the best compromise between the R_{int} , I/σ and resolution parameters for **2**. For **2**, one of two azophenyl moieties and one of four tert-butyl groups are found to be disordered over two positions with relative occupancies 0.68/0.32 and 0.64/0.36, respectively.

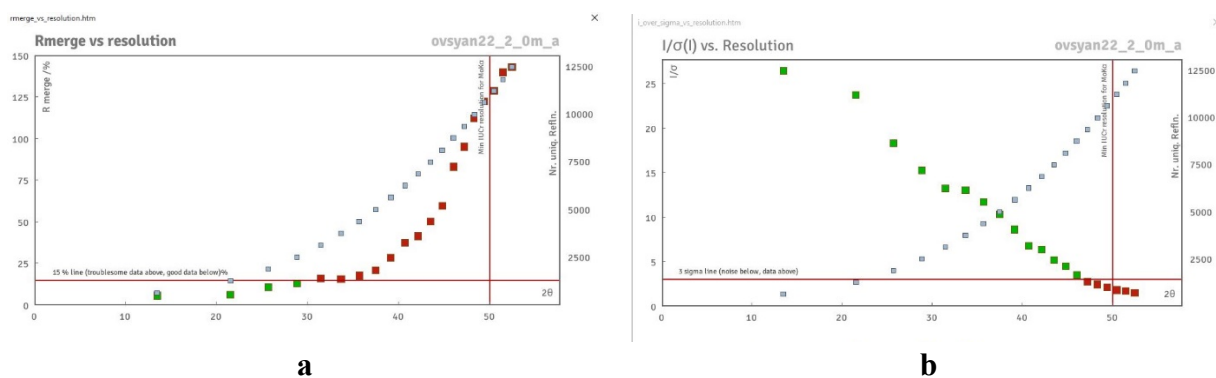


Figure SA. The comparison of R_{merge} vs Resolution (a) and I/σ vs Resolution plots (b) for **2**.

The X-ray diffraction data for **2-Dy** were obtained on the ‘Belok/XSA’ beamline ($\lambda = 0.7517$ Å, ω -scans) of the Kurchatov Synchrotron Radiation Source (Moscow, Russian Federation). Diffraction patterns were collected using Mardtb goniometer, equipped with Rayonix SX165 2D positional sensitive CCD detector at 100(2) K.^{4,5} The frames were recorded with oscillation range of 1° . The data were processed using the XDS program.¹² The multi-scan method was used for absorption correction. The structure was solved with SHELXT⁷ and refined by full-matrix least squares on F^2 using the *Olex2* software,¹³ which utilises the SHELXL⁸ module. The hydrogen atoms were placed in calculated positions and included in the refinement within the riding model

with fixed isotropic displacement parameters $U_{\text{iso}}(\text{H}) = 1.5U_{\text{eq}}(\text{O})$, $1.2U_{\text{eq}}(\text{N})$, and $1.2U_{\text{eq}}(\text{C})$. The hydrogens atoms belonging to water molecule and phenol group were refined using restraints and constraints. Due to poor quality of crystals **2-Dy**, the correction of data sets at θ_{max} was applied based on the R_{merge} vs Resolution and I/σ vs Resolution plots (see below Figure SB). The 2θ angle ranges of $1.74 \leq 2\theta \leq 22.5^\circ$ was found to be the most suitable for the structure refinement in order to find the best compromise between the R_{int} , I/σ and resolution parameters for **2-Dy**.

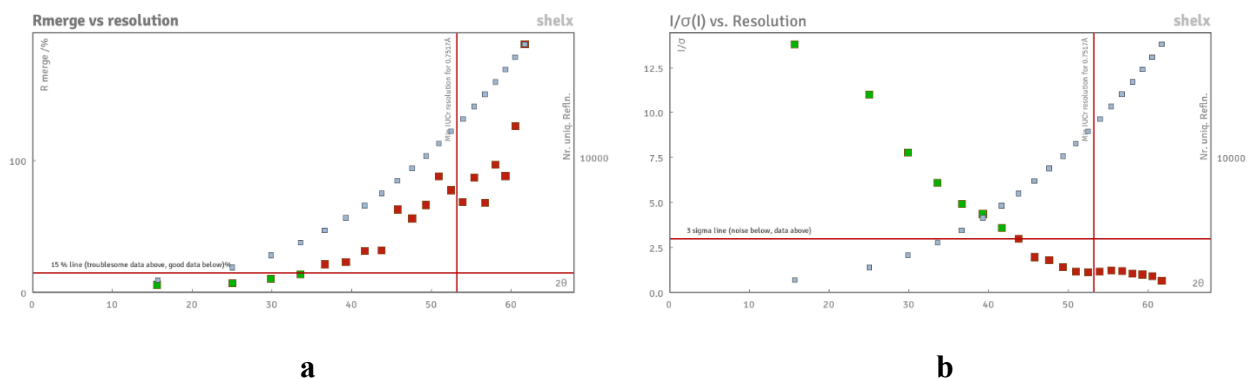


Figure SB. The comparison of R_{merge} vs Resolution (a) and I/σ vs Resolution plots (b) for **2-Dy**.

For **2-Dy** two *tert*-butyl substituents of calixarene ligand are disordered over two positions with relative occupancies 0.71/0.29 and 0.76/0.24. The position of atoms with a higher occupancy are presented on the Figures of the article. For **2-Dy**, the positions of one MeOH and H₂O solvate molecule, trapped within calix[4]arene cavity were reliably refined. Additionally, one H₂O solvent molecule, located in the void between the complex species, was found to be disordered over two positions with relative occupancies 0.5/0.5. The crystal data, X-ray diffraction experiment and the refinement parameters are gathered in Table S1.

Crystallographic data for the studied structures have been deposited in the Cambridge Crystallographic with CCDC Number 2410855 (**2**), 2442375 (**2-Dy**) and are available for free of charge downloading from <https://www.ccdc.cam.ac.uk>.

Table S1. Experimental crystallographic data, obtained for **2** and **2-Dy**.

| Compound | 2 | 2-Dy |
|-------------------------------------|--|---|
| Crystal formula | C ₇₄ H ₈₂ N ₆ O ₆ | C ₇₄ H ₇₈ DyN ₆ O ₆ , CH ₄ O, 2H ₂ O |
| Formula Weight, g·mol ⁻¹ | 1151.45 | 1379.00 |
| Crystal System | triclinic | monoclinic |
| Space group | <i>P</i> -1 | <i>P</i> 2 ₁ / <i>c</i> |
| λ , Å | 0.71073 | 0.7517 (synchrotron) |
| Temperature, K | 105 | 100(2) |
| Cell parameters | $a = 10.5440(12)\text{Å}$, $b = 16.2534(19)\text{Å}$, $c = 19.985(2)\text{Å}$; $\alpha = 90.635(4)^\circ$ $\beta = 102.105(4)^\circ$ $\gamma = 108.609(4)^\circ$ | $a = 19.127(4)\text{Å}$, $b = 13.967(3)\text{Å}$, $c = 26.635(5)\text{Å}$; $\alpha = 90^\circ$ $\beta = 96.86(3)^\circ$ $\gamma = 90^\circ$ |

| | | |
|---|--|--|
| V, Å ³ | 3162.5(6) | 7064(2) |
| Z and Z' | 2 and 1 | 4 and 1 |
| D(calc), g·cm ⁻³ | 1.209 | 1.297 |
| μ, mm ⁻¹ | 0.077 | 1.283 |
| F(000) | 1232.0 | 2868 |
| θ _{Min} /θ _{Max} , ° | 2.07 / 23.5 | 1.74 / 22.5 |
| Reflections measured | 144558 | 11960 |
| Independent reflections | 9325 | 7014 |
| Observed reflections [<i>I</i> > 2σ(<i>I</i>)] | 7141 | 4505 |
| Completeness to θ _{max} , % | 99.7 | 88.9 |
| Goodness-of-fit on F ² | 1.013 | 1.220 |
| R [<i>I</i> > 2σ(<i>I</i>)] | R ₁ = 0.0804 wR ₂ = 0.1918 | R ₁ = 0.1127, wR ₂ = 0.2708 |
| R (all reflections) | R ₁ = 0.1039, wR ₂ = 0.2091 | R ₁ = 0.1809, wR ₂ = 0.3244 |
| ρ _{max} /ρ _{min} , eÅ ⁻³ | 0.87/-0.61 | 1.99/-1.71 |

1.5.2. Checkcif report responses

For **2**, there are two alerts of B level which appear upon the checkcif report procedure. The responses are provided below:

THETM01_ALERT_3_B The value of sine(theta_max)/wavelength is less than 0.575

Calculated sin(theta_max)/wavelength = 0.5610

Response: Poor crystal quality. The correction of data set was applied at θ_{max} = 23.5

PLAT097_ALERT_2_B Large Reported Max. (Positive) Residual Density 0.87 eA-3

Response: Large Positive Residual Density at a desordered azophenyl fragment.

For **2-Dy**, there are 2 Alerts of A level and 7 Alerts of B level which appear upon the checkcif report procedure. The responses are provided below:

THETM01_ALERT_3_A The value of sine(theta_max)/wavelength is less than 0.550

Calculated sin(theta_max)/wavelength = 0.5091

PLAT029_ALERT_3_A _diffn_measured_fraction_theta_full value Low . 0.899 Why?

Response: The X-ray diffraction experiment was performed using synchrotron radiation source. Based on the *R_{merge}* vs Resolution and *I/sigma* vs Resolution plots the correction of data set was applied at θ_{max} = 22.5. The intense increase of *R_{merge}* parameter was observed above 50% at higher θ_{max}. The obtained data set quality was related with the poor crystal quality and the experimental set up at the synchrotron station.

PLAT342_ALERT_3_B Low Bond Precision on C-C Bonds 0.04292 Ang.

Response: The X-ray diffraction experiment was performed using synchrotron radiation source. Since the intense increase of *R_{merge}* parameter above 50%, the correction of data set was applied at θ_{max} = 22.5. The obtained data set quality was related with the poor crystal quality and the experimental set up at the synchrotron station.

PLAT420_ALERT_2_B D-H Bond Without Acceptor O0AA --H0AA . Please Check

PLAT420_ALERT_2_B D-H Bond Without Acceptor O0AA --H0AB . Please Check

PLAT420_ALERT_2_B D-H Bond Without Acceptor O1AA --H1AA . Please Check

Response: This is a disordered water molecule.

PLAT420_ALERT_2_B D-H Bond Without Acceptor O8 --H8C . Please Check

PLAT420_ALERT_2_B D-H Bond Without Acceptor O8 --H8D . Please Check

Response: This O(08) atom is attributed to accommodated within the calix[4]arene hydrophobic cavity water molecule, which is involved in H-bonding with OH-phenolic group of calix[4]arene platform. As a result, the H-atoms of water molecule are orientated outwardly the cavity. Additionally, the water molecule is shielded by tert-butyl substituents, disposed on the upper rim of the macrocycle.

PLAT911_ALERT_3_B Missing FCF Refl Between Thmin & STh/L= 0.509 784 Report

1 1 0, 3 3 0, 3 4 0, 4 2 0, 5 1 0, 12 9 0,
12 10 0, 14 9 0, -13 9 1, -12 8 1, -10 7 1, -10 9 1,
-9 2 1, -9 4 1, -9 6 1, -8 3 1, -8 5 1, -7 2 1,
-7 3 1, -7 5 1, -5 3 1, -4 2 1, -1 1 1, 2 4 1,
3 3 1, 3 4 1, 4 2 1, 4 3 1, 4 7 1, 5 3 1,
6 5 1, -13 9 2, -8 4 2, -8 6 2, -8 10 2, -5 3 2,
-5 4 2, -4 0 2, -4 2 2, -3 0 2, -3 2 2, -3 3 2,
-2 0 2, -2 5 2, -1 0 2, 2 1 2, 2 3 2, 3 2 2,
3 3 2, 3 4 2, 4 2 2, 5 0 2, 10 10 2, 10 11 2,
-8 5 3, -8 8 3, -7 5 3, -6 3 3, -6 5 3, -6 6 3,
-6 8 3, -5 1 3, -4 2 3, -3 3 3, -2 1 3, -1 5 3,
0 1 3, 1 1 3, 4 2 3, 8 4 3, 10 9 3, -12 5 4,
-11 4 4, -9 4 4, -8 4 4, -7 0 4, -6 0 4, -5 0 4,
-5 6 4, -4 0 4, -4 1 4, -4 2 4, -3 0 4, -3 3 4,
-2 0 4, -2 1 4, -2 3 4, -1 0 4, -1 1 4, -1 3 4,
0 0 4, 0 1 4, 0 3 4, 1 0 4, 1 1 4, 1 3 4,

Response: The X-ray diffraction experiment was performed using synchrotron radiation source. Based on the R_{merge} vs Resolution and I/σ vs Resolution plots the correction of data set was applied at $\theta_{max} = 22.5$. The intense increase of R_{merge} parameter was observed above 50% at higher θ_{max} . The obtained data set quality was related with the poor crystal quality and the experimental set up at the synchrotron station.

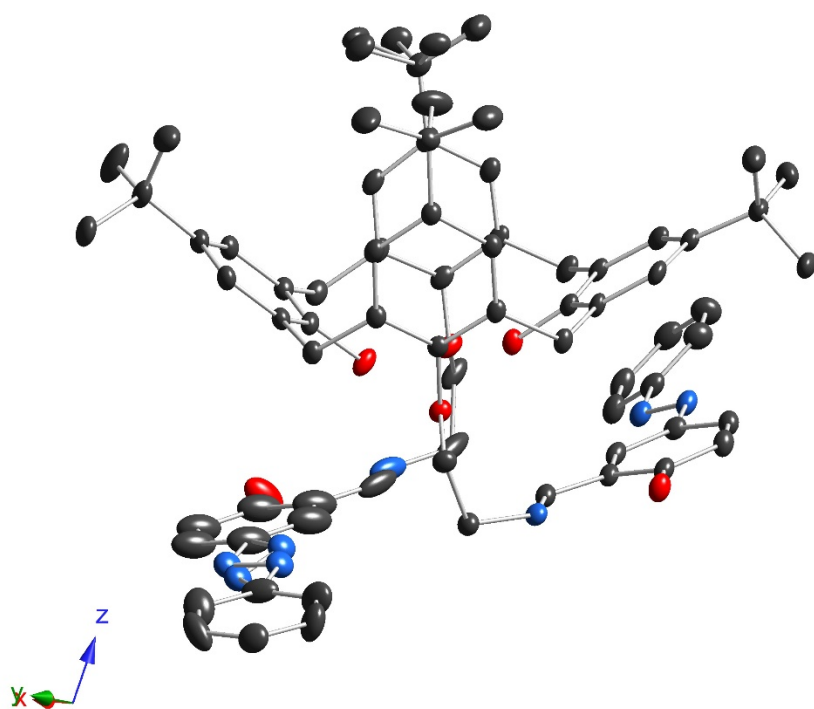
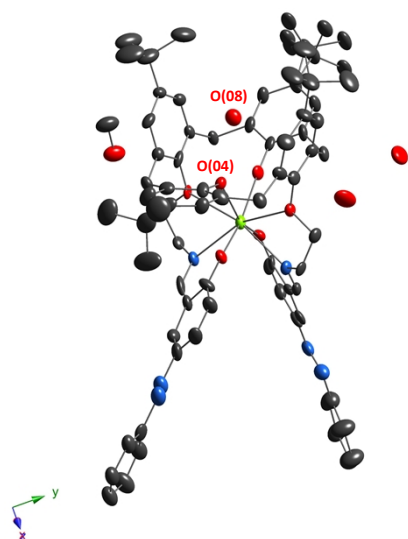
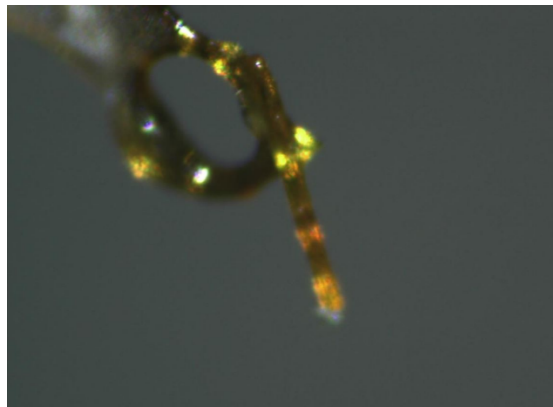


Figure S4. ORTEP view for asymmetric parts of **2**, showing thermal ellipsoids at the 30% probability level. The C-, O-, and N- atoms are presented as dark grey, red, and blue ellipsoids, respectively. The H-atoms are omitted for clarity.



a



b

Figure S5. ORTEP view for asymmetric part of **2-Dy** (a), showing thermal ellipsoids at the 30% probability level. The C-, O-, N- and Dy-atoms are presented as dark grey, red, blue and light green ellipsoids (a). The photo of the studied crystal of **2-Dy** (b), showing its needle-like morphology.

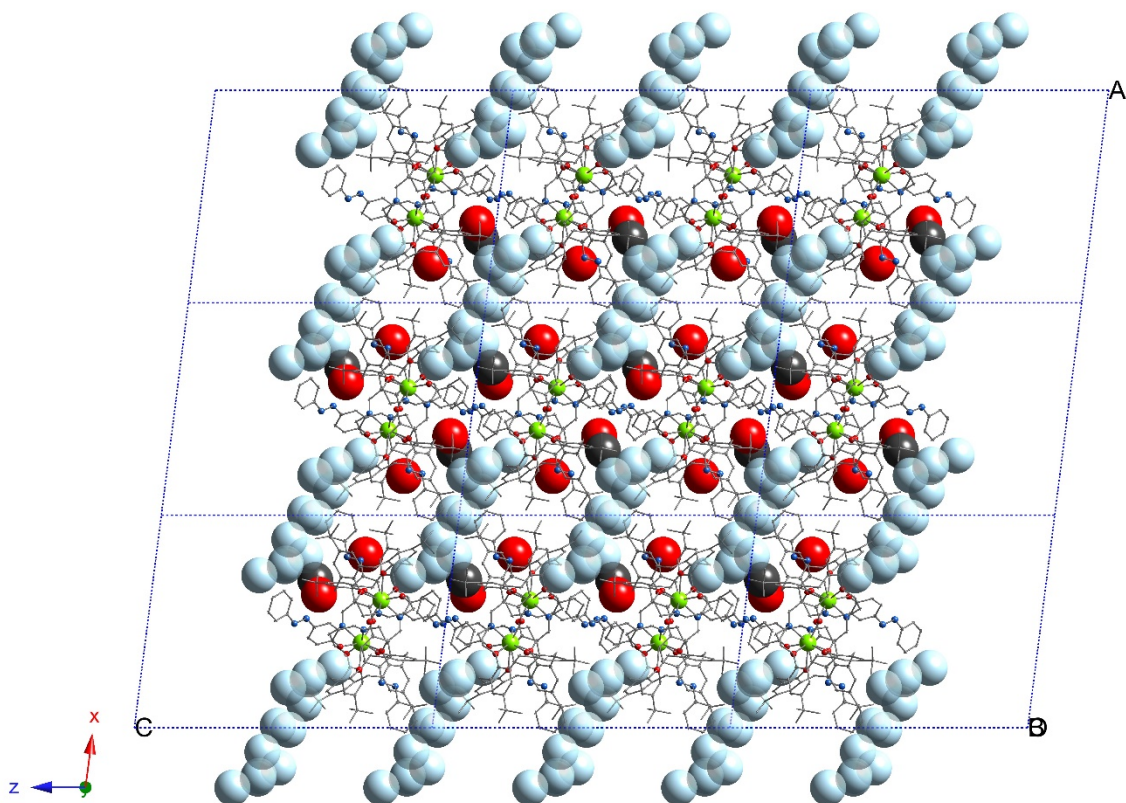


Figure S6. For **2-Dy**, a fragment of crystal packing, showing the formation of voids between the complex species. The O-, N- and Dy-atoms are presented as red, blue and light green spheres. The H-atoms are omitted for clarity. The H₂O and MeOH are presented in spacefill mode. The voids are depicted as light blue spheres.

Table S2. The general geometrical characteristics obtained for **2**.

| | |
|--|--|
| Dihedral angle between the opposite aryl unit of calix[4]arene backbone | 13.5(3) ° 113.2(3) ° |
| Intramolecular H-bonding between the phenolic moieties and adjacent O-ether junctions belonging to calix[4]arene backbone | $d_{O(25)...O(28)} = 2.837(4) \text{ \AA}$ $d_{O(27)...O(59)} = 3.007(4) \text{ \AA}$ |
| Intramolecular H-bonding within appended salicylideneamine moieties | $d_{O(63)...N(60)} = 2.585(6) \text{ \AA}$ $d_{O(48)...N(45)} = 2.583(4) \text{ \AA}$ |
| D-H-A angles for intramolecular H-bonding within the salicylideneamine moieties | $\angle O(48)-H(48)-N(45) = 149.0(4)^\circ$ $\angle O(63)-H(63) N(60) = 148.8(8)^\circ$ |
| D...A length for hypothetical intermolecular H-bonding between the salicylideneamine moieties, belonging to adjacent calix[4]arene molecules | $d_{O(63)...N(45)} = 3.011(7) \text{ \AA}$ $d_{O(48)...N(60)} = 3.083(6) \text{ \AA}$ |
| D-H-A angle for hypothetical intermolecular H-bonding between the salicylideneamine moieties, belonging to adjacent calix[4]arene molecules | $\angle O(48)-H(48)-N(60) = 80.7(4)^\circ$ $\angle O(63) H(63) N(45) = 78.3(4)^\circ$ |
| Salicylideneamine moieties bond lengths | |
| $d(C-N), \text{ \AA}$ | 1.290(9) 1.295(5) |
| $d(C-C), \text{ \AA}$ | 1.391(6) 1.435(7) 1.428(6) 1.430(5) |
| $d(C-O), \text{ \AA}$ | 1.338(7) 1.310(5) |
| Azophenyl moieties bond lengths | |
| $d(C_{Ar}-N_{azo}), \text{ \AA}$ | 1.44(1) 1.508(9) 1.48(1) 1.49(2) 1.432(5) 1.427(5) |
| $d(N_{azo}-N_{azo}), \text{ \AA}$ | 1.24(2) 1.29(1) 1.257(5) |
| Azophenyl moieties torsion angles | |
| $\angle (C_{Ar}-C_{Ar}-N_{azo}-N_{azo}), ^\circ$ | -8(1) 1.0(9) -9.8(6) -16.1(4) -15(1) 11(1) |

Table S3. *SHAPE* analysis¹⁴ for Dy(III) atom in **2-Dy**.

| | | | | | | | | | | | | |
|--------|--------|--------|-------|--------|--------------|--------|----------|---------|--------|-------|-------|---------|
| OP-8 | HPY-8 | HBPY-8 | CU-8 | SAPR-8 | TDD-8 | JGBF-8 | JETBPY-8 | JBTPR-8 | BTPR-8 | JSD-8 | TT-8 | ETBPY-8 |
| 33.150 | 20.228 | 11.017 | 5.878 | 2.536 | 2.490 | 13.360 | 25.045 | 4.346 | 3.941 | 6.419 | 6.730 | 20.981 |

| Label | Shape | Symmetry |
|----------|--|----------|
| OP-8 | Octagon | D_{8h} |
| HPY-8 | Heptagonal pyramid | C_{7v} |
| HBPY-8 | Hexagonal bipyramid | D_{6h} |
| CU-8 | Cube | O_h |
| SAPR-8 | Square antiprism | D_{4d} |
| TDD-8 | Triangular dodecahedron | D_{2d} |
| JGBF-8 | Johnson - Gyrobifastigium (J26) | D_{2d} |
| JETBPY-8 | Johnson - Elongated triangular bipyramid (J14) | D_{3h} |
| JBTP-8 | Johnson - Biaugmented trigonal prism (J50) | C_{2v} |
| BTPR-8 | Biaugmented trigonal prism | C_{2v} |
| JSD-8 | Snub disphenoid (J84) | D_{2d} |
| TT-8 | Triakis tetrahedron | T_d |
| ETBPY-8 | Elongated trigonal bipyramid (see 8) | D_{3h} |

Table S4. Comparison of the coordination bond lengths for Ln(III) coordination spheres in similar **2-Dy** and earlier reported La-complex.¹⁵

| | 2-Dy | La-complex |
|-------------|-------------|------------|
| d (Ln-N), Å | 2.49(2) | 2.643(6) |
| | 2.50(2) | 2.672(4) |
| d (Ln-O), Å | 2.24(2) | 2.398(4) |
| | 2.28(2) | 2.360(6) |
| | 2.51(1) | 2.732(4) |
| | 2.45(2) | 2.335(5) |
| | 2.55(1) | 2.692(4) |
| | 2.15(1) | 2.350(4) |

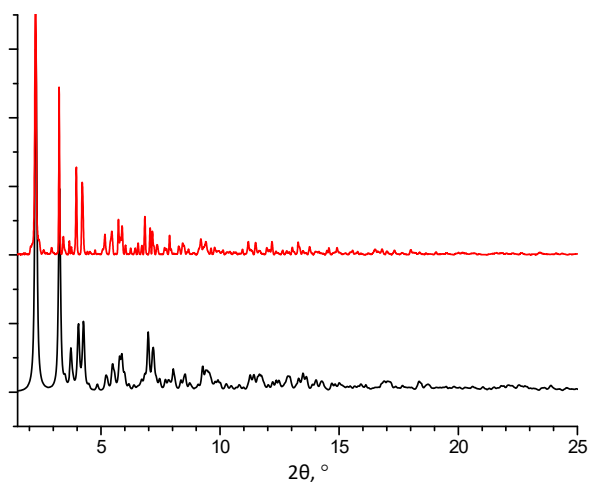


Figure S7. For **2-Dy**, a comparison of experimental powder X-ray diffraction pattern (up) with the simulated one (bottom), demonstrating a good matching, obtained using synchrotron radiation.

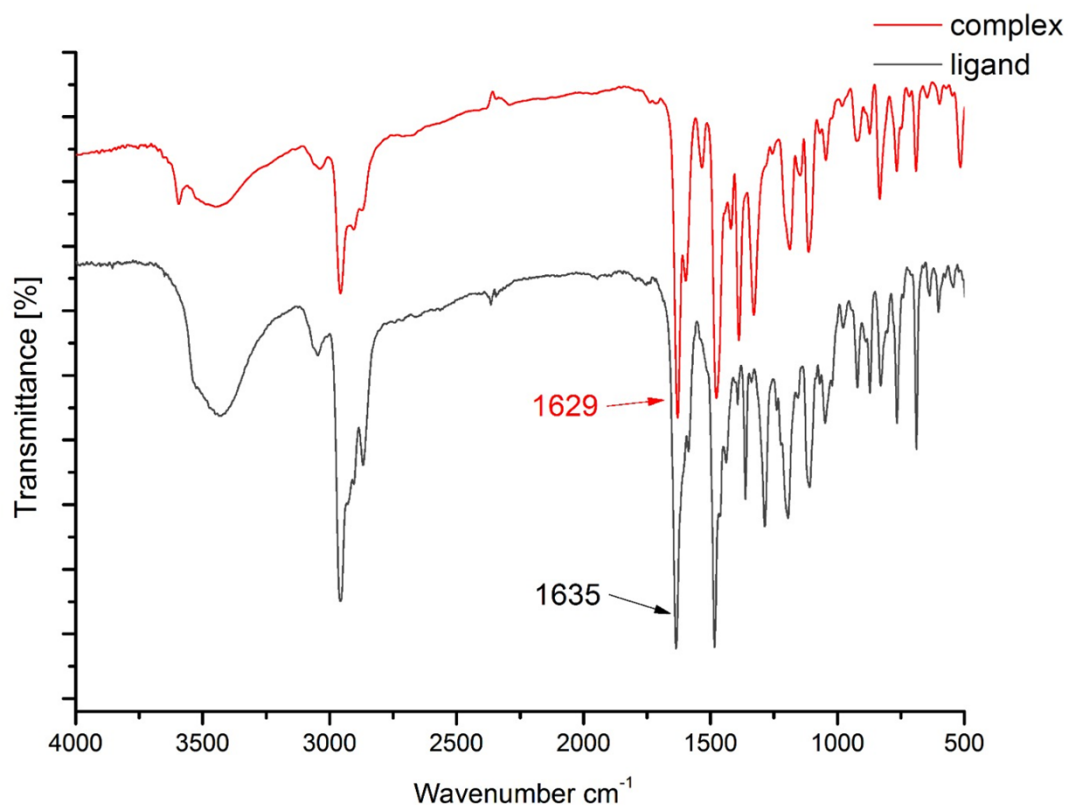


Figure S8. Comparison of IR spectra for **2** (black curve) and **2-Dy** (red curve).

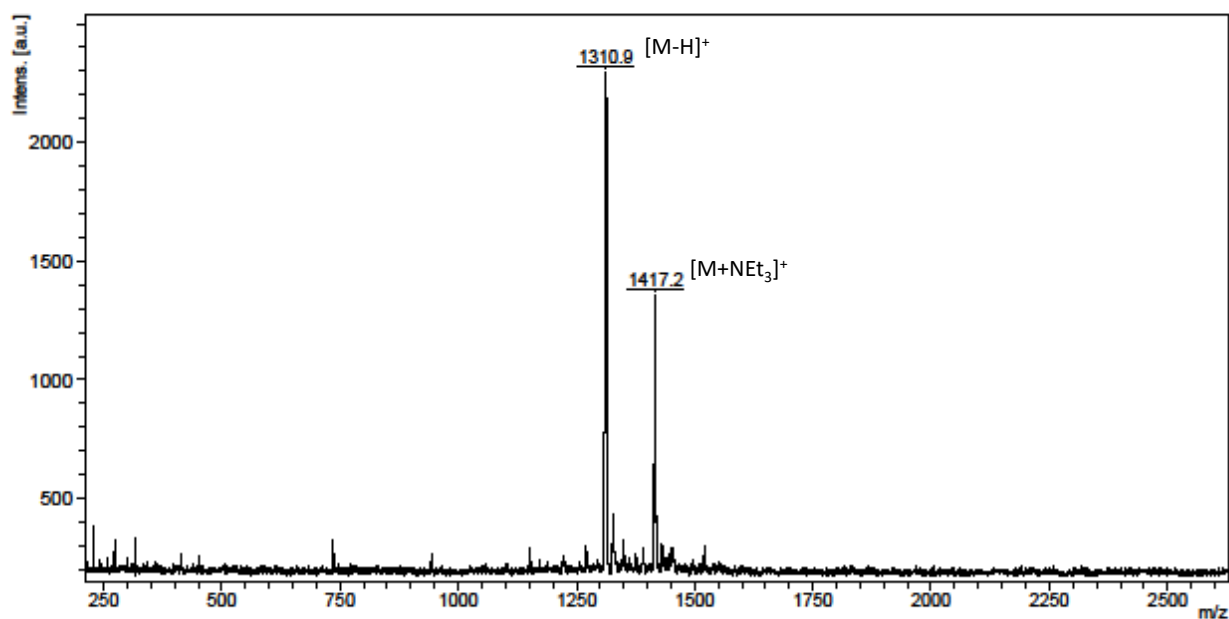


Figure S9. MALDI TOF-MS spectrum for **2-Dy**.

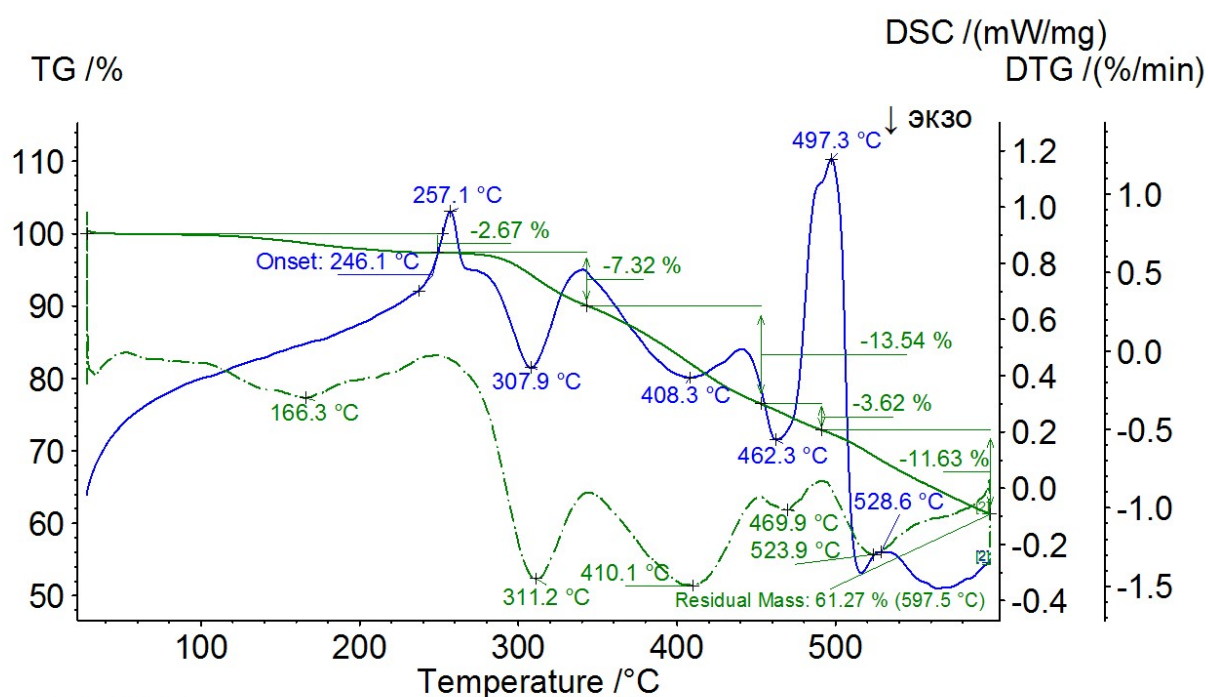


Figure S10. TGA/DSC traces for **2-Dy**. The mass-loss of the air-dried powdered sample in the temperature range from 25 till 260 °C corresponds to 2.67 wt %, which may be consistent with the release of one trapped within the calix[4]arene macrocyclic cavity H₂O molecule and one H₂O molecule presenting in the voids of crystal packing.

2. SQUID magnetometry study

Magnetic measurements were obtained with a Quantum Design SQUID magnetometer MPMS-XL. Direct current (dc) susceptibility measurements were carried out over the temperature range of 1.8–300 K under an applied dc field of 5000 Oe. Magnetization measurements were made at low temperatures with applied dc fields in the range of $-45\text{...}45$ kOe. Alternating current (ac) susceptibility measurements were measured under zero dc and 500 Oe applied dc field with 3.5 G oscillating ac field in the frequencies range from 0.1 to 1488 Hz. Measurements were performed on polycrystalline samples. The ground powder was restrained in Apiezon grease. The magnetic data were corrected for the sample holder.

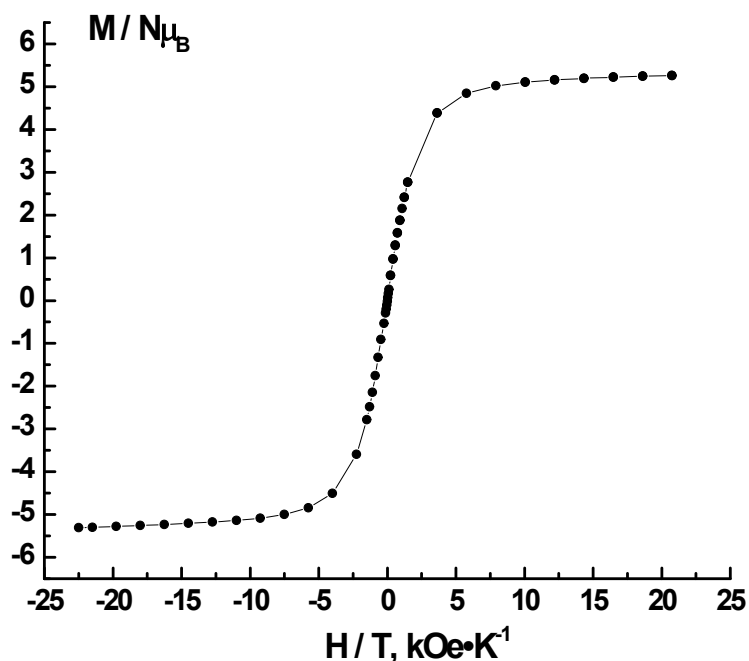


Figure S11. Field dependence of magnetization for 2-Dy at 2 K.

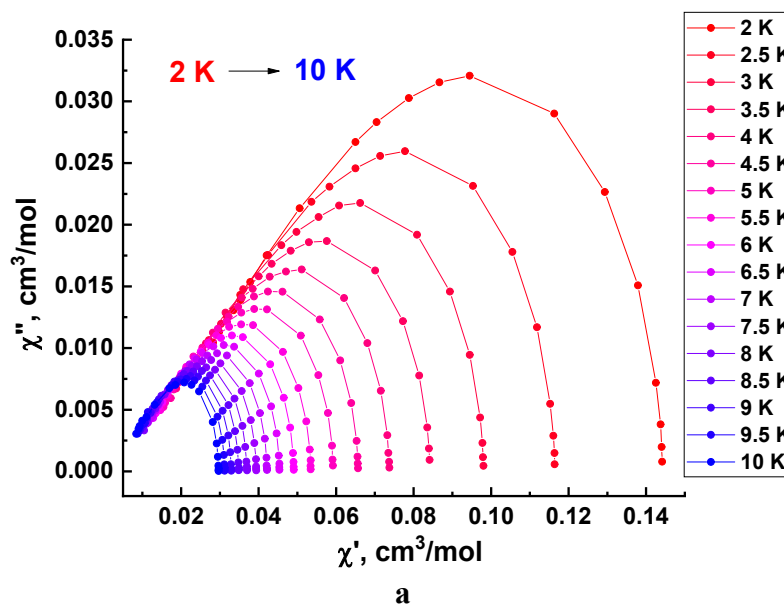


Figure S12. The $\chi''(\chi', T)$ dependences obtained under a zero dc-field applied.

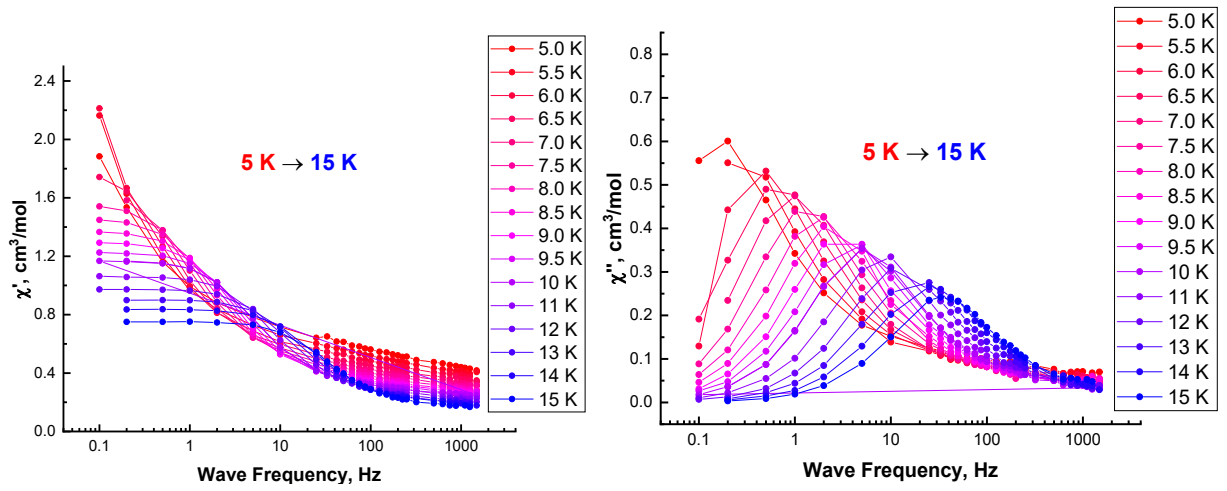


Figure S13. The temperature dependence of $\chi'(\nu)$ and $\chi''(\nu)$ magnetic susceptibility at 500 Oe dc-field applied.

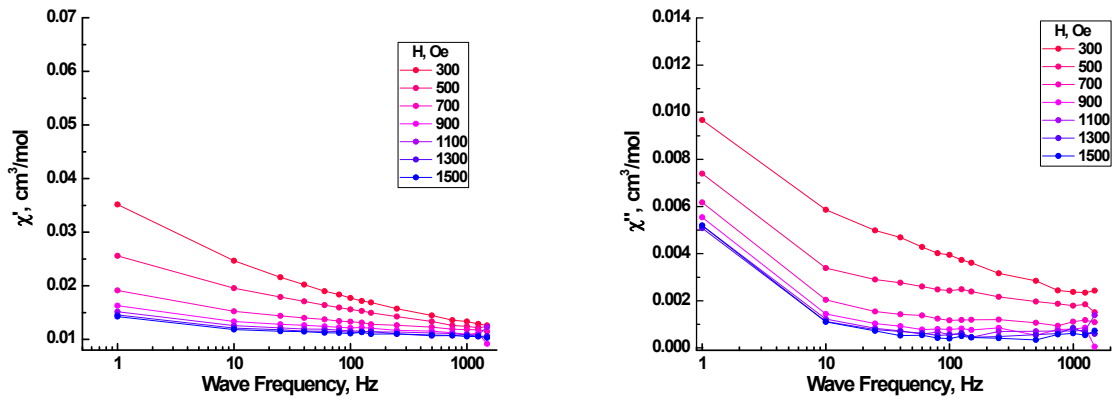


Figure S14. Frequency dependencies of $\chi'(\nu)$ and $\chi''(\nu)$ magnetic susceptibility at 4.5 K and different applied dc magnetic fields.

The analysis of frequency dependences ($\chi'(\nu)$, $\chi''(\nu)$) in the absence and at 500 Oe dc magnetic field was performed using the Debye model, presented below. The calculated values of relaxation time were gathered in the Tables S5 and S6.

$$\chi'(\nu) = \chi_s + (\chi_T - \chi_s) \cdot (1 + (\nu\tau)^{1-\alpha} \cdot \sin(\pi\alpha/2)) / (1 + 2(\nu\tau)^{1-\alpha} \cdot \sin(\pi\alpha/2) + (\nu\tau)^{2-2\alpha})$$

$$\chi''(\nu) = (\chi_T - \chi_s) \cdot ((\nu\tau)^{1-\alpha} \cdot \cos(\pi\alpha/2)) / (1 + 2(\nu\tau)^{1-\alpha} \cdot \sin(\pi\alpha/2) + (\nu\tau)^{2-2\alpha}).$$

Table S5. The calculated relaxation times depending on temperature at a zero dc magnetic field applied.

| T, K | τ , s |
|------|-------------------|
| 2 | 0.0043 ± 0.0002 |
| 2.5 | 0.0041 ± 0.0002 |
| 3 | 0.0040 ± 0.0002 |
| 3.5 | 0.0039 ± 0.0002 |
| 4 | 0.0037 ± 0.0002 |
| 4.5 | 0.0036 ± 0.0002 |
| 5 | 0.0034 ± 0.0002 |
| 5.5 | 0.00314 ± 0.00016 |
| 6 | 0.00301 ± 0.00015 |
| 6.5 | 0.00290 ± 0.00014 |
| 7 | 0.00276 ± 0.00013 |
| 7.5 | 0.00259 ± 0.00013 |
| 8 | 0.00251 ± 0.00012 |
| 8.5 | 0.00235 ± 0.00012 |
| 9 | 0.00223 ± 0.00011 |
| 9.5 | 0.00214 ± 0.00010 |
| 10 | 0.00200 ± 0.00010 |

Table S6. The calculated relaxation times depending on temperature at 500 Oe dc magnetic field applied.

| T, K | τ , s |
|------|-----------------------|
| 5 | 1.12 ± 0.17 |
| 5.5 | 0.75 ± 0.30 |
| 6 | 0.33 ± 0.06 |
| 6.5 | 0.215 ± 0.012 |
| 7 | 0.154 ± 0.008 |
| 7.5 | 0.105 ± 0.020 |
| 8 | 0.075 ± 0.19 |
| 8.5 | 0.0575 ± 0.0023 |
| 9 | 0.0441 ± 0.0016 |
| 9.5 | 0.0337 ± 0.0012 |
| 10 | 0.0263 ± 0.0007 |
| 11 | 0.0172 ± 0.0004 |
| 12 | 0.0115 ± 0.0003 |
| 13 | 0.00822 ± 0.00016 |
| 14 | 0.00587 ± 0.00011 |
| 15 | 0.00434 ± 0.00007 |

References

- 1 H. G. Becker, W. Berger, G. Domschke, ORGANIKUM. Organisch-chemisches Grundpraktikum, Deutscher Verlag der Wissenschaften, Berlin, 1965.
- 2 C. D. Gutsche, M. Iqbal, D. Stewart, Calixarenes. 19. Syntheses procedures for p-tert-butylcalix[4]arene, *J. Org. Chem.*, 1986, **51**, 742. DOI: 10.1021/jo00355a033
- 3 A.P. Luk'yanenko, E.A. Alekseeva, S.S. Basok, A. V. Mazepa, A. I. Gren'. *Russ. J. Org. Chem.*, 2011, **47**, 527–529. DOI: 10.1134/S1070428011040105
- 4 V. A. Lazarenko, P. V. Dorovatovskii, Y. V. Zubavichus, A. S. Burlov, Y. V. Koshchienko, V. G. Vlasenko, V. N. Khrustalev, *Crystals*, 2017, **7**, 11, 325. <https://doi.org/10.3390/cryst7110325>
- 5 R. D. Svetogorov, P. V. Dorovatovskii, V. A. Lazarenko, *Crystal Research and Technology*, 2020, **55**, 5, 1900184. <https://doi.org/10.1002/crat.201900184>
- 6 R. D. Svetogorov, Dionis—Diffraction Open Integration Software, Kurchatov Institute, Moscow, Russia, 2018
- 7 M. R. Ganjali, Z. Memari, R. Dinarvand, F. Faridbod, P. Norouzi, Uranyl Plasticized Membrane Sensor Based on a New Calix[4]arene, *Sens. Lett.*, 2009, **7**, 6, 1156–1162. DOI: 10.1166/sl.2009.1253
- 8 APEX2 (Version 2.1), SAINTPlus, Data Reduction and Correction Program (Version 7.31A), Bruker AXS Inc., Madison, Wisconsin, USA, 2006
- 9 G. M. Sheldrick, SADABS, Program for empirical X-ray absorption correction, Bruker-Nonius, 2004.
- 10 G. M. Sheldrick, *SHELXT* – Integrated space-group and crystal-structure determination, *Acta Crystallogr. Sect. A*, 2015, **71**, 3–8. DOI: 10.1107/S2053273314026370
- 11 G. M. Sheldrick, Crystal Structure Refinement with SHELXL, *Acta Cryst. Sect. C*, 2015, **71**, 3–8. DOI: 10.1107/S2053229614024218
- 12 W. Kabsch, *Acta Crystallogr.*, 2010, **D66**, 125. <https://doi.org/10.1107/S0907444909047337>
- 13 O. V. Dolomanov, L. J. Bourhis, R. J. Gildea, J. A. K. Howard, H. J. Puschmann, *Appl. Cryst.*, 2009, **42**, 339. <https://doi.org/10.1107/S0021889808042726>
- 14 M. Llunell, D. Casanova, J. Cirera, J. M. Bofill, P. Alemany, S. Alvarez, M. Pinsky, D. Avnir, *SHAPE, version 2.3*, University of Barcelona, Barcelona, Spain, and Hebrew University of Jerusalem, Jerusalem, Israel, 2013.
- 15 E. Bartalucci, A. A. Malär, A. Mehnert, J. B. Kleine Büning, L. Günzel, M. Icker, M. Börner, C. Wiebeler, B. H. Meier, S. Grimme, B. Kersting, T. Wiegand, *Angew. Chem. Int. Ed.*, 2023, **62**, e202217725. <https://doi.org/10.1002/anie.202217725>